Chemical, mineralogical and petrographic characterization of Roman ancient hydraulic concretes cores from Santa Liberata, Italy, and Caesarea Palestinae, Israel

Gabriele Vola[1,*], Emanuele Gotti[1], Chris Brandon[2], John P. Oleson[3] and Robert L. Hohlfelder[4]

[1] CTG Italcementi Group, Lab Dept., Via Camozzi, 124 - 24121 Bergamo, Italy
[2] Pringle Brandon Architects, 10 Bonhill St, London, EC2A 4QJ, UK
[3] Departmentt of Greek and Roman Studies, University of Victoria, Victoria BC V8W 3P4, Canada
[4] Departmentt of History, University of Colorado, Boulder, CO 80309-0234, USA
*Corresponding author: *g.vola@itcgr.net*

Abstract

This study reports chemical, mineralogical and petrographic characterization of ancient hydraulic concretes from the Roman piers at Santa Liberata Orbetello (Grosseto) Italy (~ 50 B.C.), and breakwaters at the harbour of Caesarea Palestinae, Israel (c. 25 B.C.), drilled by the ROMACONS (Roman Maritime Concrete Study) team in 2003-2005. Both sets of concrete contain a pozzolanic sanidine- and clinopiroxene-bearing tuff, identified as coming from the pyroclastic deposits of the Phlegrean Fields (Naples), the so-called *pulvis Puteolanus* of Vitruvius. However, the content of tuff changes, being predominant at Santa Liberata, whereas it is only a smaller fraction of the total aggregate at Caesarea that is mostly composed of local *kurkar* calcareous sandstone, with occasional ceramic fragments. The cementitious binding matrix presents amorphous gel-like, silica-rich C-A-S-H, with subordinated "sparry" calcite cement, and unusual dull white grains composed of calcite, tobermorite, and ettringite, apparently derived from reaction with hydrated lime in seawater. Saline encrustations, from the diffusion of chlorides and sulphates, and characteristic authigenic spherical zeolites with the "rosette" texture also occur within the mortar's porosity. These new data put further constraints on the various reactions occurring in roman concretes in over two thousand years of curing in an aggressive marine environment.

Key words: Ancient Roman harbours; hydraulic seawater concretes; pozzolanic mortars; *pulvis Puteolanus* of Vitruvius; ROMACONS project; Neapolitan Yellow Tuff (NYT).

Introduction

The Romans have used pyroclastic rocks as coarse aggregate and/or fine gravel- to fine sand-sized mortar pozzolan since the 3rd Century B.C.; all these materials are generally designed as "tuff-ash materials". These tuff-ash materials mainly come from the Phlegrean Fields,

Vesuvius and Albani hills (Bianchi et al., 2011; Bianchi and Meneghini, in press; Branton and Oleson, 1992, Oleson and Branton, 1992; Collepardi et al., 2009; Jackson and Marra, 2006; Jackson et al., 2007; 2010a; 2010b; Oleson et al., 2004; 2006; 2010). These different volcanic sources can be straightforwardly discriminated as a function of their chemical signatures, as well as by textural and mineralogical characteristics (Bernardi et al., 1982; De Rita et al., 1988; Massazza, 1974; Massazza and Costa, 1979; Jackson et al., 2010c, in press). Among them, the Phlegrean Fields tuff-ash materials were probably the most important source for the ancient roman concretes, as also historically supported by the Vitruvius' descriptions of pozzolan, the *pulvis Puteolanus* from Baia and the Bay of Naples (Oleson et al., 2004; Brandon et al., 2005). These latter pozzolanic deposits frequently consist of unconsolidated to welded pyroclastic products ascribed to the Neapolitan Yellow Tuff (NYT), a large eruption dating ~ 15.000 yr before present (de' Gennaro et al., 2000) (Figure 1).

In order to further study the Roman concretes in maritime settings, i.e. to characterise the formulation of these ancient technical materials, their physical properties, their placement and provenance, in the 2001 was established the ROMACONS - Roman Maritime Concrete Study. Standard core drilling procedures had been adopted in order to take intact stratigraphic samples (0.09 m in diameter and up to 5.8 m long) which were then analysed in the laboratories of CTG Italcementi with a comprehensive set of physical, mechanical, chemical and mineralogical protocols. Since 2002, the team has recovered cores at Portus, Anzio, Cosa, Santa Liberata, Baia, and Egnazia in Italy, at the harbours of Caesarea in Israel, Alexandria in Egypt, Chersonisos in Crete, and finally at Soli-Pompeiopolis near Mersin in Turkey in 2009 (Figure 2) (Oleson et al., 2004; 2006; Brandon et al., 2005; 2008; 2010;

Hohlfelder et al., 2007; Vola et al., 2010a; 2010b). These studies have confirmed that the Roman engineers extensively used pozzolanic tuff-ash materials from pyroclastic deposits as the optimal ingredient for hydraulic concrete in maritime structures both in Italy and elsewhere in the Mediterranean, even in Israel (Branton and Oleson, 1992; Hohlfelder et al., 2007) or at Crete (Brandon et al., 2005). The extensive use of pozzolanic materials by Romans has been corroborated in 2004 by the ROMACONS team with the construction of an about 8 m^3 experimental *pila* in the harbour of Brindisi, by mixing the lime-based mortar with a pozzolanic powdered tuff-ash from Bacoli, Pozzuoli, near Naples; they used the same tuff-ash uncrushed, as the concrete aggregate, casting the *pila* in seawater within an appropriate formwork. The resulting concrete was very similar to the ancient ones from a chemical and a physical-mechanical perspective (Hohlfelder et al., 2005; Oleson et al., 2006; Gotti et al., 2008; see Table 1), even if the microstructural fabric was apparently somewhat different (Jackson et al., 2010a, in press).

Here, in the frame of the ROMACONS project, we extend the previous studies on Roman ancient hydraulic concretes by characterising several cores sampled at Santa Liberata, Grosseto, Italy, and Caesarea Palestinae, Israel; the obtained data were compared with those of the tuff-ash coarse aggregate recently quarried at Bacoli, on the outskirts of Pozzuoli, Naples, to identify the provenance of raw materials used to cast these two ancient concretes.

Location and sampling procedure of Santa Liberata and Caesarea Palestinae cored concretes

In order to fully characterize the aggregate and the mortar portions, cores were taken at different depths. In the following, the location and description of the analyzed samples are reported.
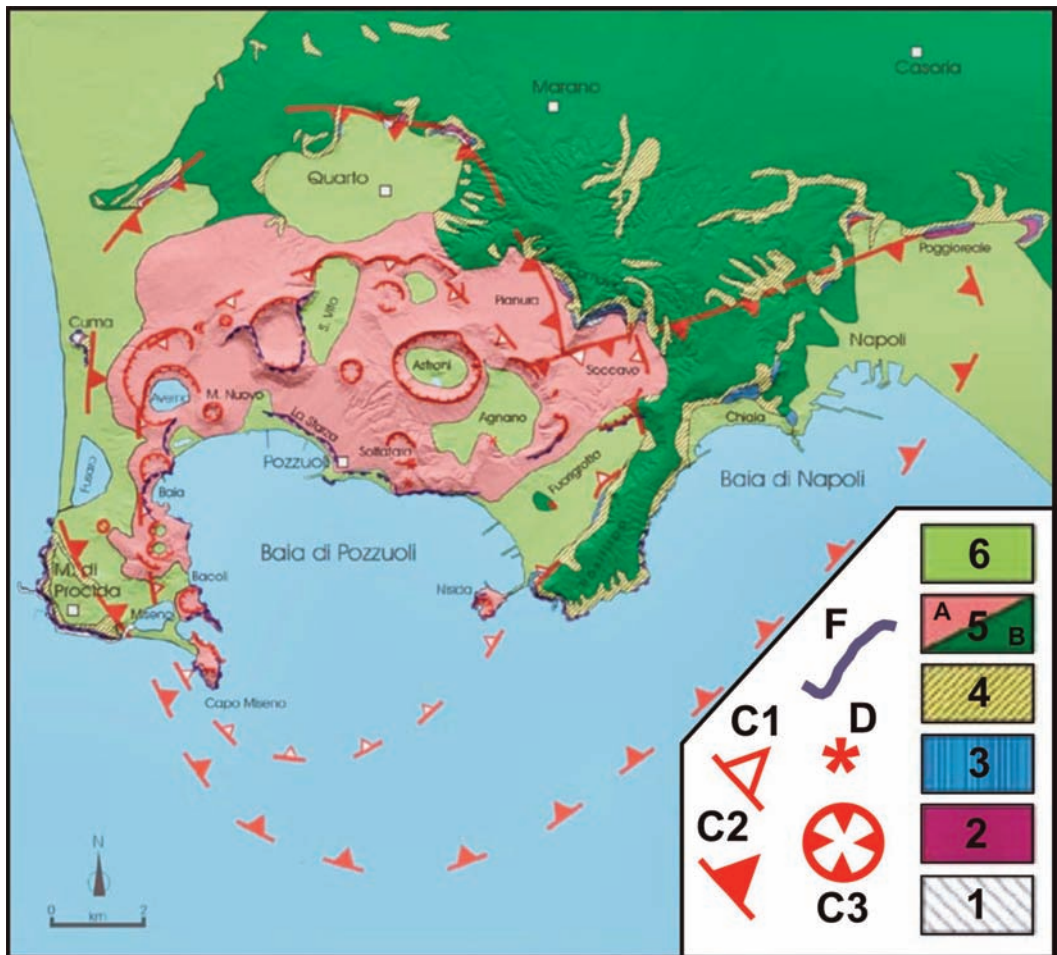
Figure 1. A: Geological and structural sketch map of Phlegrean Fields deposits. Map symbols: 1: volcanic deposits older than 39 kyr; 2: Campanian Ignimbrite 37 kyr; 3: volcanic products erupted between 39 and 15 kyr; 4: Neapolitan Yellow Tuff (NYT) (15 kyr); 5: volcanic products younger than 15 kyr, 5a: surge and flow proximal deposits; 5b: falling distal deposits; 6: recent plain sediments; C1: Neapolitan Yellow Tuff caldera (12 kys); C2: Campanian Ignimbrite caldera (37 kys); C3: craters younger than 12 kys; D: lava domes; F: cliffs. From http://www.ov.ingv.it/volcanology/libretto/capitolo3c.htm.

Off the headland at Santa Liberata on the Argentario peninsula, four large Roman concrete piers (Latin: *pilae*) were built in the sea on the western side of the fishpond below a Roman villa. Two of these blocks are set onto the shoreline while the other two are isolated. A core sample labeled SLI.03 with a length of 1.50 m was taken from the top of pier closest to the fishpond.

A second core at Santa Liberata with a length of 5.80 and a diameter of 0.09 m, named SLI.04, was drilled vertically down through the middle of an exceptionally well preserved pier, located
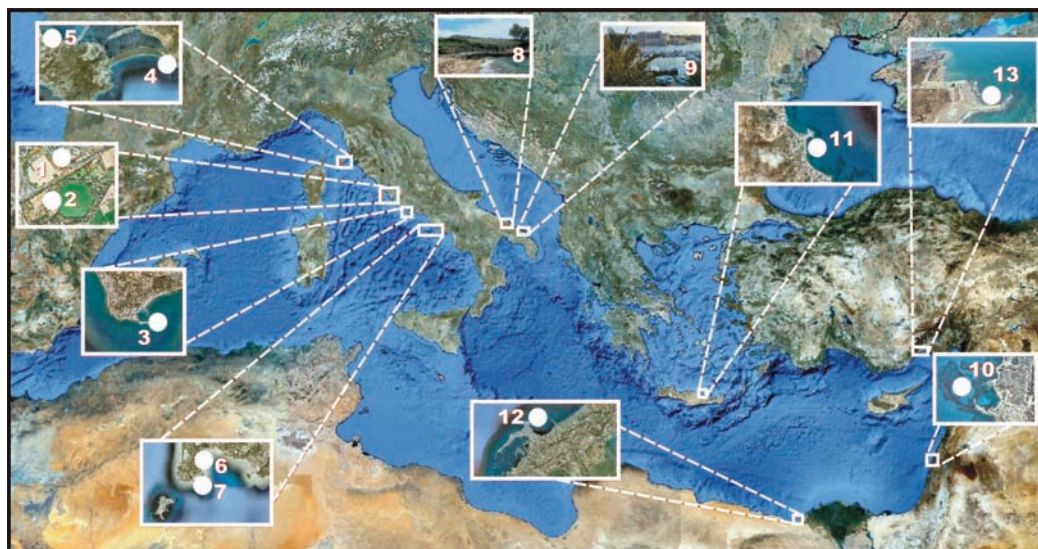
Figure 2. Ancient Roman concrete harbours, investigated by the ROMACONS Team, along the Mediterranean coast. 1-2: Portus Claudius, ~ 50 B.C., and Portus Traianus, ~.115 B.C., at Ostia (Rome); 3: Portus Neronis, ~ 60 B.C., at Anzio (Rome); 4: Portus Cosanus, ~ 60 B.C., at Ansedonia, Orbetello (Grosseto); 5: fishpond and pier at Santa Liberata, Orbetello (Grosseto); 6: Portus Iulius and Portus Baianus, mainly 1st century B.C., at Baia, Pozzuoli (Naples); 7: quarry of pozzolanic tuff-ash aggregates at Bacoli, Phlegrean Volcanic Fields, Pozzuoli (Naples); 8: Egnatia, probably first century B.C. at Torre Egnazia (Brindisi); 9: modern reproduction of Vitruvius's pier at the harbour of Brindisi; 10: harbour Sebastos breakwaters at Caesarea Palestinae, Israel; 11: Chersonisos harbour, 1st century B.C.-1st century A.D., Crete (Greece); 12: Alexandria harbour, 1st century B.C., Egypt; 13: Soli-Pompeiopolis harbour, near Mersin, Turkey, 1st century B.C. (photos: Gabriele Vola and Corrado Stanislao).

Table 1. Chemical analysis and physical-mechanical tests of Brindisi experimental concrete (BRI.05) vs Santa Liberata (SLI.04). Si/Al and Ca/Si ratios, alkali content, values of Young's modulus, and compressive strength are from Gotti et al. (2008).

Cores	BRI.05-A	BRI.05-B	BRI.05-C	SLI.04-A	SLI.04-B	SLI.04-C
Sample	mortar	mortar	mortar	mortar	mortar	mortar
Si/Al	3.6	3.6	3.6	3.3	-	-
Ca/Si	0.3	0.4	0.5	0.3	-	-
Na_2O (%)	2.8	2.8	2.6	3.1	-	-
K_2O (%)	6.0	5.6	5.3	4.7	-	-
Length (mm)	125	204	205	190	200	200
Diameter (mm)	85	85	85	85	85	85
Density (kg/m^3)	1530	1390	1415	1550	1523	1526
Young's Modulus (MPa)	5740	3730	3880	6940	6280	6040
Compressive strength (MPa)	7.2	3.9	3.5	8.5	8.1	7.5

at about 70 m to the west of the fishpond. This pier measures approximately 9 x 9 x 8 m (its height is variable) and its upper surface is now comprised between 0.5 m and 1.5 m below sea level. In order to determine the possible vertical variation of this concrete, the core was projected to sample all the pier whole height; however, the core barrels were not sufficient to reach the bottom of the block, since even after all six of the 1.0-meter long barrels had been fitted and drilled into the concrete, the ancient seabed was not reached. Nevertheless, the extremely long sample recovered provides a unique data on deep water ancient concreting (Oleson et al., 2006).

In order to study the concrete three portions of this core were sampled at depths of 185-223 cm (SLI.04-A), 380-400 cm (SLI.04-B) and 535-555 cm (SLI.04-C) from the top end.

Concrete cores from Caesarea Palestinae were drilled and sampled by the ROMACONS team in October 2005. Five cores (CAE.05-1, CAE.05-2, CAE.05-3, CAE.05-4, CAE.05-5) were taken from the enormous harbour of Sebastos (the Greek equivalent of Augustus), built by King Herod of Judea in approximately 23 to 15 B.C. This harbour represents the largest artificial harbour ever built in the open sea up to that time. Four cores were extracted from some submerged concrete blocks – the structural elements of the southern breakwater – and one from the terminus of the northern breakwater that defines the eastern face of the harbour mouth (Hohlfelder et al., 2007). The CAE.05-1 core was recovered from the southern breakwater at a depth on top of block of 3.5 m. It is composed of four fragments and its length is 1.10 m. Coring stopped when wood was encountered, probably a horizontal tie beam, without loss of material. The top of the core was covered with marine encrustations. The CAE.05-2 core was recovered from a block on the southern breakwater at depth on top of block of 3.0 m. It is composed of five solid joining fragments, and its length is 1.65 m. The coring appeared to have penetrated the entire block, since the coring tube began to run easily before coring was terminated. There was no apparent loss of core, and the upper and lower ends are darker green because moist from exposure to sea water. The CAE.05-3 third core was recovered from the northwest corner of the block on northern breakwater at a depth on top of block of 3 m. It is ca. 0.80 m long, but most of it was crumbly, and the proportion recovered was ca. 60%. The core was very fragmentary, either because of the softness of the concrete, or as a result of the action of the coring barrel, which jammed several times in the top 0.10 m. The longest fragment of 0.15 m is mostly composed of the *kurkar* aggregate. Portions of the core seem to have come loose from the mortar during the extraction process only to be ground up by the core bit. The CAE.05-4 fourth core was recovered from the southern breakwater, at a depth on top of block of 3 m. It is composed of nine fragments, and his length is 2.10 m. The proportion recovered is 91.3%. The coring penetrated through to the lower surface of the block, and there seemed to have been some loss of material at the crumbly section between -1.5 to - 1.8 m. There were marine encrustations on both the top and bottom of the core. Finally, the CAE.05-5 last core is from the area on southern breakwater at a depth on top of block of 2.5 m, and its length is 1.95 m. The proportion recovered was 97.5%. The irregularity of the upper surface of the block, along with a strong surge, made mounting of the coring frame very difficult. Coring was slowed by the hardness of the *kurkar* aggregate, and by fragmentation of the upper 0.03 m of the block, which jammed the corer.

Analytical methods

The concrete core boxes of the ROMACONS project were stored and subsequently analyzed at the CTG Italcementi laboratory in Bergamo; in Figure 3 an example of stored cores is reported.

Concrete slices, cut using a diamond wire,

Figure 3. A-B: core boxes and 9 cm sized concrete slices from Santa Liberata (SLI.03 and SLI.04), and Caesarea Palestinae (CAE.05-4 and CAE.05-5). Core boxes are stored at CTG Italcementi Lab. Dept. in Bergamo; C: macrograph from SLI.03 core.

were first investigated with a stereomicroscope, for a preliminary visual inspection; a pointed tool was adopted to scratch some grams of the fine-grained aggregate (esp. pumiceous scoria, tuff-ash fragments, black shards, and white grains of reacted lime), and the binding cementitious matrix for further chemical and mineralogical characterization (see below). Some of these slices of the concrete and of the tuff aggregate from Bacoli were also selected to prepare polished thin sections for the petrographic examination with the BX51 Olympus polarized microscope and with the Leo Scanning Electron Microscope (SEM), equipped with a Sirius Energy Dispersive Spectrometer (EDS).

The bulk chemical features were obtained with the X-Ray Fluorescence (XRF) spectroscopy method, using a Panalytical cubiX X-Ray Fluorescence spectrometer with the following conditions: M.h.T. = 50 kV and M.a.c. = 4 mA; in addition, chlorides content, calcimetry and acid attack were carried out with the Florentin method (see the Italian standard UNI 6505:1973).

X-Ray Powder Diffraction (XRPD) analysis was performed with a Bruker D8-advance X-ray diffractometer, operating with a parafocusing geometry, equipped with cuKa radiation, two sets of soller slits and a lynxeye™ PsD Detector. All XRPD spectra were collected between 5-70° of 2θ with a step of 0.02° per second.

Finally, the pore-size distribution and the total porosity were determined by the mercury intrusion porosimetry method.

Results and discussion

Visual inspection of cores

Preliminary mesoscopic inspections were carried out on wet concretes to increase the contrast between aggregates and the binding matrix.

SLI.03 core shows a greenish grey to dark greenish grey mortar, with rounded grains of grey/green tuff aggregate, occasional fragments of limestone, and many white clasts of reacted lime. The aggregate consists of large irregular chunks of yellow brown tuff 10 dm sized,

containing many lighter yellow inclusions of fibrous pumice and clasts of hard black shards (Figure 3C). The color of the tuff fades to a greenish tinge near its junction with mortar. One piece of limestone aggregate is visible at -0.10 to -0.20 m, very hard and fine-grained, light grey to pale yellow (Oleson et al., 2004).

SLI.04 core is composed of large, brown tuff aggregate and well-compacted mortar. Initial examination of the core has revealed that the proportion of mortar to aggregate seems to be less in the lower and upper third of the block than in the central third. The coarse tuff aggregate shows a vacuolar appearance, earthy consistency, ochre yellow to brown green color, up to 20 cm sized, and consists of vitreous tuff-ash matrix with pumice clasts, black shards, lava fragments and phenocrysts. The mortar is also pozzolan-based, with tuff-ash fragments, dark aggregates, ceramics, the so-called *cocciopesto*, and white dull clasts of reacted lime into the seawater. The binding matrix appears microcrystalline and grey colored.

CAE.05 cores contain two different coarse aggregates: large porous limestone fragments up to 20 cm sized, and subordinated up to 7 cm sized white clasts of reacted lime. The former were probably quarried locally from calcarenite *kurkar* deposits in outcrops throughout the region that lie in ridges parallel to the modern shoreline. The latter are poorly mixed clasts of reacted lime, showing particular black-and-white stripes. The mortar is strongly enriched in pozzolanic materials, including tuff-ash and lava fragments; white grains of reacted lime, calcareous sandstone *kurkar* aggregates, ceramics, and wood fragments, probably deriving from the original frameworks also occur. The binding matrix looks like microcrystalline and grey colored.

Chemical analysis of tuff-ash materials and mortars

Bulk chemical analyses of tuff-ash aggregates from Santa Liberata (SLI.03 and SLI.04), Bacoli (BAC.04) and mortars from Santa Liberata (SLI.04-A) and Caesarea (CAE.05-1, CAE.05-2, CAE.05-3, CAE.05-4, CAE.05-5) are reported in Table 2. Similar distribution of major elements attests that the provenance of pozzolanic tuff-ash materials is probably the same, and that formulations adopted to cast both the concretes, were not so different, as well.

Similarity between Santa Liberata and Caesarea mortars is also ascribed to the content of calcite, which represents an important product of reaction. However, the samples CAE.05-2 and CAE.05-3 show a different chemical composition with respect all the other mortars (Table 2); the former sample has the lowest content of SiO_2 and the highest of CaO, whereas the latter sample has the lowest amount of CaO and the highest of MgO. Probably, the CAE.05-2 was prepared with an higher amount of lime, whereas the CAE.05-3 underwent a stronger alteration by seawater.

Soluble silica and insoluble residue both evidence that pozzolanic reactions have been occurred. Moreover, the high value of the hydraulic index (H.I.), defined as (SiO_2 wt. % + Al_2O_3 wt. % + Fe_2O_3 wt. %) / (CaO wt. %+ MgO wt. %), attests that both mortars are properly hydraulic materials (Table 2).

Mineralogical and petrographic analysis of the aggregate

The concrete coarse-grained aggregate (4 mm-20 cm) and a large part of the mortar fine-grained aggregate (d < 4 mm) in Santa Liberata cores are composed of a yellow brown vitric tuff-ash. This pozzolanic material consists of pumiceous clasts, dark glassy shards, lava fragments with primary phenocrysts and secondary weathering minerals, surrounded by a vitreous fine-ash matrix (Figure 4 A, B). Pumice clasts are generally rounded or flat in shape, with amygdaloidal vesicles and a glassy composition, that apparently gives to this material a strong reaction with the hydrated lime. This explains the characteristic reaction rims that

Table 2. Columns 1-3: XRF bulk chemical analysis (%) of pozzolanic tuff-ash aggregates from Santa Liberata and Bacoli and mortars from Santa Liberata and Caesarea. Calcimetry of mortars from Santa Liberata and Caesarea are also reported (%).

Cores	SLI.03	SLI.04	BAC.04	SLI.04-A	CAE.05-1	CAE.05-2	CAE.05-3	CAE.05-4	CAE.05-5
Samples	tuff-ash	tuff-ash	tuff-ash	mortar	mortar	mortar	mortar	mortar	mortar
Depth (cm)	-	155	-	380-400	40-100	20-80	-	80-150	190-220
SiO_2	52.5	51.7	52.5	40.9	41.7	34.9	38.3	42.3	39.7
Al_2O_3	16.3	16.0	15.5	12.2	11.9	10.4	9.0	12.6	11.6
Fe_2O_3	3.9	4.1	3.4	3.3	2.5	2.3	2.1	2.6	2.5
CaO	3.7	1.2	2.4	12.2	15.5	20.9	6.3	12.4	15.7
MgO	1.0	1.8	0.8	2.4	1.8	2.2	17.5	4.2	3.9
SO_3	0.0	0.1	<0.06	0.3	1.0	1.4	1.6	0.4	1.1
Na_2O	5.5	6.6	3.3	3.1	3.3	2.9	2	3.5	3.1
K_2O	7.9	6.8	7.9	4.7	4.1	2.9	1.9	4.6	3.7
SrO	0.0	0.0	0.0	0.1	0.0	0.0	0.0	0.0	0.0
Mn_2O_3	0.1	0.1	0.1	0.1	0.1	0.1	0.1	0.1	0.1
P_2O_5	0.1	0.1	0.1	0.1	0.1	0.1	0.1	0.1	0.1
TiO_2	0.4	0.4	0.4	0.3	0.3	0.3	0.2	0.3	0.3
Cl-	-	-	-	1.1	0.9	1.0	1.4	0.9	1.0
L.O.I.	8.6	11.0	13.4	19.2	16.7	20.7	19.4	15.9	16.9
$CaCO_3$	-	-	-	8.8	11.8	12.0	12.0	10.5	8.8
S.S. %	-	-	-	7.9	12.3	16.0	1.1	9.3	12.0
I.R. %	-	-	-	48.7	36.7	24.6	41.1	44.4	35.4
S.S. / I.R.	-	-	-	0.2	0.3	0.7	0.0	0.2	0.3
H.I.	15.7	24.4	22.3	3.9	3.2	2.1	2.1	3.5	2.7

L.O.I.: Loss On Ignition; S.S.: Soluble Silica; I.R.: Insoluble Residue; H.I.: Hydraulic Index, defined as: (SiO_2 wt. % + Al_2O_3 wt. % + Fe_2O_3 wt. %) / (CaO wt. % + MgO wt. %).

often blur gradually into the surrounding cementitious binding paste. Sometimes also a reddish halo is present, which derives from the opaque inclusion of alteration. Characteristic amygdaloidal vesicles are filled-in with fibrous zeolites; XRPD analyses (see Table 3) on pumice and tuff-ash clasts confirm the typical association of phillipsite plus chabazite both in SLI.03 and SLI.04. Dark glassy mm-sized shards with network of polygonal cracks are probably the result of sudden cooling of primary pyroclastic fragments. Distinguishing features on thin section are the yellowish color on plane polarized light (PPL), and the non birefringence on crossed polarizers (XPL). The XRPD data (see Table 3) of a black shard extracted in SLI.04.A shows the wide bump of the amorphous phase, overlapped by characteristic peaks of calcite, phillipsite and chabazite, as secondary weathering minerals. Volcaniclastic rocks fragments with porphyritic texture and microcrystalline groundmass are also very common. Primary phenocrysts are generally K-feldspar and clinopyroxene, with subordinated plagioclase, opaque minerals, and secondary analcime. K-feldspar is often longed and
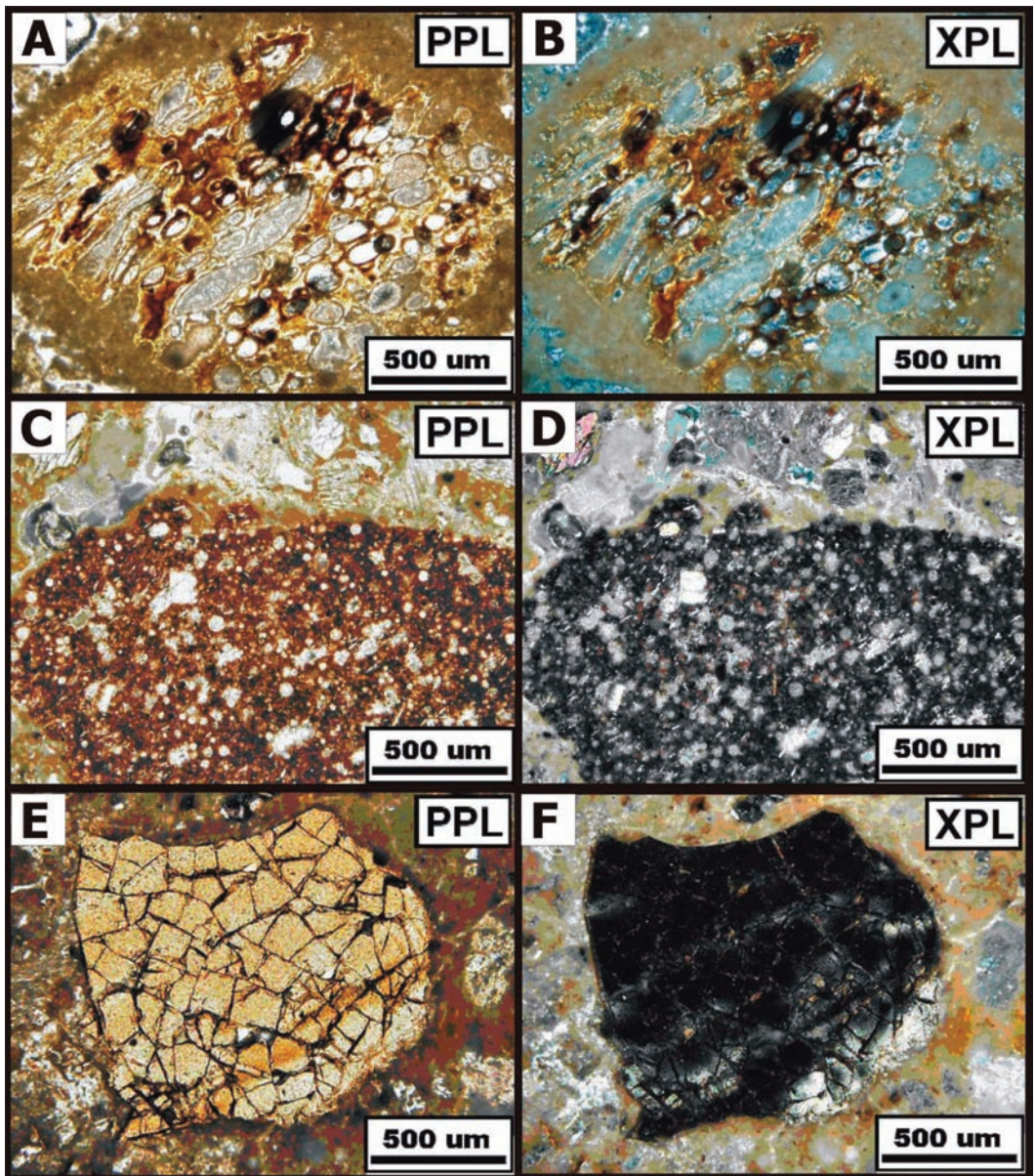
Figure 4. Characteristic components of the coarse pozzolanic tuff-ash aggregates from SLI.03, SLI.04 and CAE.05. A-B: Pumiceous vitric clast with vesicles filled in of zeolites and microcrystalline reaction rim (PPL and XPL); C-D: lava fragment composed of analcime phenocrysts, likely derived from leucite, and skeletal plagioclase scattered within a microcrystalline opaque groundmass (PPL and XPL); E-F: black shard, the so-called obsidian, with network of cooling cracks (PPL and XPL).

Table 3. Mineralogical association determined by XRPD analysis of ancient mortars.

Cores	Specimens	Predominant seawater cements phases	Subordinate seawater cements phases	Pozzolanic aggregate primary crystals and secondary alteration	Non pozzolanic aggregate
SLI.03	Mortar	Cal	Gp + Vat	San + Ana + Phi	Ms
SLI.04-A	Mortar	Cal	Cha + Vat	San + An + Ana	Clc + Ill
CAE.05-1	Mortar	Cal + Tbm	Phi + Cha	San + Ana	Cal + Qtz + Ill
CAE.05-2	Mortar	Cal + Tbm	Phi + Etr + Bsn	San + Ana	Cal + Ill
CAE.05-2	Mortar	Cal	Tbm + Etr + Hl + Phi	San + Ana	Qtz + Ill
CAE.05-3	Mortar	Cal	Phi	San + Cpx + Ana	Qtz + Ath + Ill
CAE.05-4	Mortar	Cal	Phi + Cha	San + Cpx + Ana	Qtz + Ill
CAE.05-5	Mortar	Cal + Tbm	Phi	San + Cpx + Ana	Cal + Ill
SLI.03	Binding matrix	Cal	Phi + Cha + Br	San + Ana	Kfs + Ill
CAE.05-3	Binding matrix	Cal	Mg-Cal + Hl + Sj	San + Ana + Phi	Qtz + Ill
SLI.03	White clast	Cal + Tbm	Phi + Br + Hl	-	-
SLI.03	White clast	Cal + Gp	Vat	-	-
SLI.04-C	White clast	Tbm + Etr	Cal + Hyc + Vat	-	-
CAE.05-2	White clast	Cal	Tbm + Etr	-	Qtz
CAE.05-3	White clast	Mg-Cal	Cal	-	-
SLI.04-A	Black shard	-	-	Cal + Phi + Cha	-
SLI.03	Tuff-ash	-	Cal + Tbm	San + Ana + Phi + Cha	-
SLI.03	Tuff-ash	-	Gp + Cal	Phi + Cha	-
SLI.03	Tuff-ash	-	Cal + Mg-Cal	San + Ana + Phi + Cha	Ill
SLI.04-A	Tuff-ash	-	Cal + Hyt	San + Ana + An + Clc	-
SLI.04-A	Tuff-ash	-	Cal + Mg-Cal + Hl	San + Ana + Phi + Cha	Ill
SLI.04-B	Tuff-ash	-	Cal + Hyt	San + Ana + An + Clc	-
SLI.04-C	Tuff-ash	-	Cal + Hyt	San + Ana + An + Clc	-
CAE.05-2	Tuff-ash	-	Cal + Tbm + Hl	San + Phi	Ill
CAE.25-2	Pumice	-	-	San + Ana + Phi + Cal	-
BAC.04	Tuff-ash	-	-	San + Ana + Phi + Cha	-

Seawater cement phases include: Br: Brucite; Bsn: Bassanite; Cal: Calcite; Cha: Chabazite; Etr: Ettringite; Gp: Gypsum; Hl: Halite; Hyc: Hydrocalumite; Hyt: Hydrotalcite; Mg-Cal: Magnesium Calcite; Phi: Phillipsite; Sj: Sjogrenite; Tbm: Tobermorite; Vat: Vaterite. Volcanic pozzolan includes tuff pumice, lava and crystal fragments, and their weathering products: An: Anorthite; Ana: Analcime; Cha: Chabazite; Cpx: Clinopyroxene; Phi: Phillipsite; San: Sanidine. Sedimentary sands and non pozzolanic aggregates include: Ath: Antophyllite; Cal: calcite; Clc: Clinochlore; Kfs: K-feldspar; Ill: Illite; Ms: muscovite; Qtz: Quartz.

twinned, sometimes with chemical zonation and spongy texture (Figure 5). Clinopyroxene presents stubby prismatic habit, typical cleavage at 90°, yellowish or olive green color and weak pleochroism on plane polarized light (PPL), and second order bright interference colors under crossed polarizers (XPL). As far as the lava fragments groundmass, the variolitic texture is predominant, characterized by domains of fanning intergrowths of skeletal plagioclase and dendritic clinopyroxene. K-feldspar and clinopiroxene phenocrysts are also scattered within the binding cementitious paste in the mortar. In this case, they probably represent insoluble remains of a dissolved, unconsolidated, fine, powdery natural grain size distribution of the vitric-crystal volcanic ash, or remains from a powdered pozzolanic material, already dissolved, perhaps obtained by builders with a mechanical grinding of the volcanic tuff-ash aggregate (Figure 5). Fine-grained ceramics, the so-called *cocciopesto*, also occur within the mortar with the typical microcrystalline reddish matrix (Figure 6 A-B), composed of iron oxides, with accidental scattered grains of quartz. Finally, wood fragments, and benthonic foraminifera occur within the mortar too (Figure 6 C-D-E-F). The former came from the original formwork, the latter were probably included in the mortar with marine sediments.

The concrete coarse-grained aggregate in Caesarea cores is composed of sandstone fragments (4 mm-20 cm) from the *kurkar* eolianite local deposit, which generally presents calcareous and fossiliferous grainstones-packstones with gastropods, bivalves, foraminifera, and detritic quartz. This cemented Pleistocene sediment is a beachrock that outcrops along the Mediterranean coastal cliffs of Israel (Sneh et al., 1998).

As regards the mortar, fine-grained aggregate (d < 4mm) in Caesarea cores is strongly enriched in pozzolanic yellow brown tuff aggregates, as well.

Petrographic examinations coupled with XRPD analyses (Table 3) of tuff-ash and pumice clasts show a similar composition as those of Santa Liberata. The characteristic mineralogical association consists of sanidine and clinopiroxene, as primary volcanic minerals, with analcime and phillipsite as secondary alterations. The most important difference between Caesarea and Santa Liberata, is that lava fragments, black shards and ceramics are extremely subordinated to the tuff-ash and pumice clasts in the Caesarea mortars, as compared with Santa Liberata mortars.

The tuff-ash aggregate from Bacoli (BAC.04) is composed of a pale yellow orange aggregate, quite compacted, even if the porosity percentage, detected with mercury intrusion porosimetry, is very high, ∼ 54%. The pore size shows a characteristic bimodal distribution (Figure 7). The distinguishing feature in thin section is the characteristic pyroclastic texture, composed of partially vitreous fine ash passing to cryptocrystalline matrix, in which fibrous, vesicular and glassy pumices, lava and crystal fragments are accidentally scattered (Figure 8). The color of the tuff-ash is brown in plane polarized light (PPL), while it is generally opaque under crossed polarizers (XPL). Vesicles of pumice clasts are filled-in with zeolitic minerals, and show typical longed tabular fluidal textures (Figure 8). Lava fragments often show longed, prismatic, and simple-twinned K-feldspar (probably sanidine), with subordinated prismatic clinopyroxene, and pine-needle plagioclases in the groundmass. XRPD spectra presents amorphous phase, plus phillipsite and chabazite as secondary weathering minerals. K-feldspar and analcime, deriving from lava fragments, are subordinated (Table 3).

The similarity of chemical (Table 2), mineralogical (Table 3) and textural features between aggregates hosted in the Santa Liberata and Caesarea concretes with those of the Bacoli deposit demonstrated that aggregates are
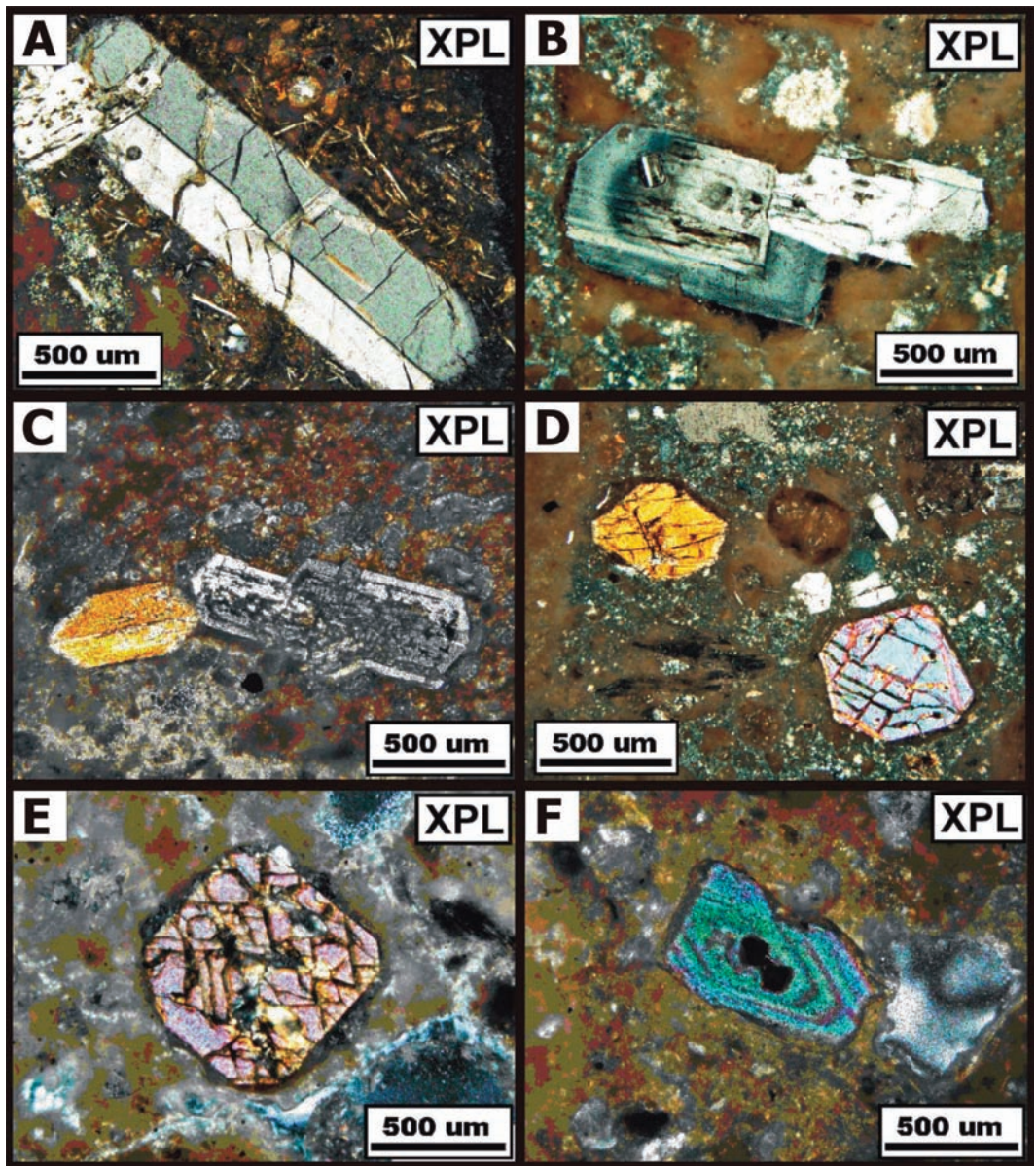
Figure 5. Characteristic phenocrysts of the fine pozzolanic tuff-ash aggregates from SLI.03, SLI.04 and CAE.05. A: Twinned and longed K-feldspar, probably sanidine, within a microcrystalline lava fragment; B: spongy zoned K-feldspars within a vitric tuff-ash; C: spongy zoned feldspars and stubby twinned clinopyroxenes within a pumiceous clast; D-E: stubby clinopyroxene crystals with characteristic 90° cleavage within the mortar; F: stubby and clepsydra zoned clinopyroxene. (All photos in XPL).
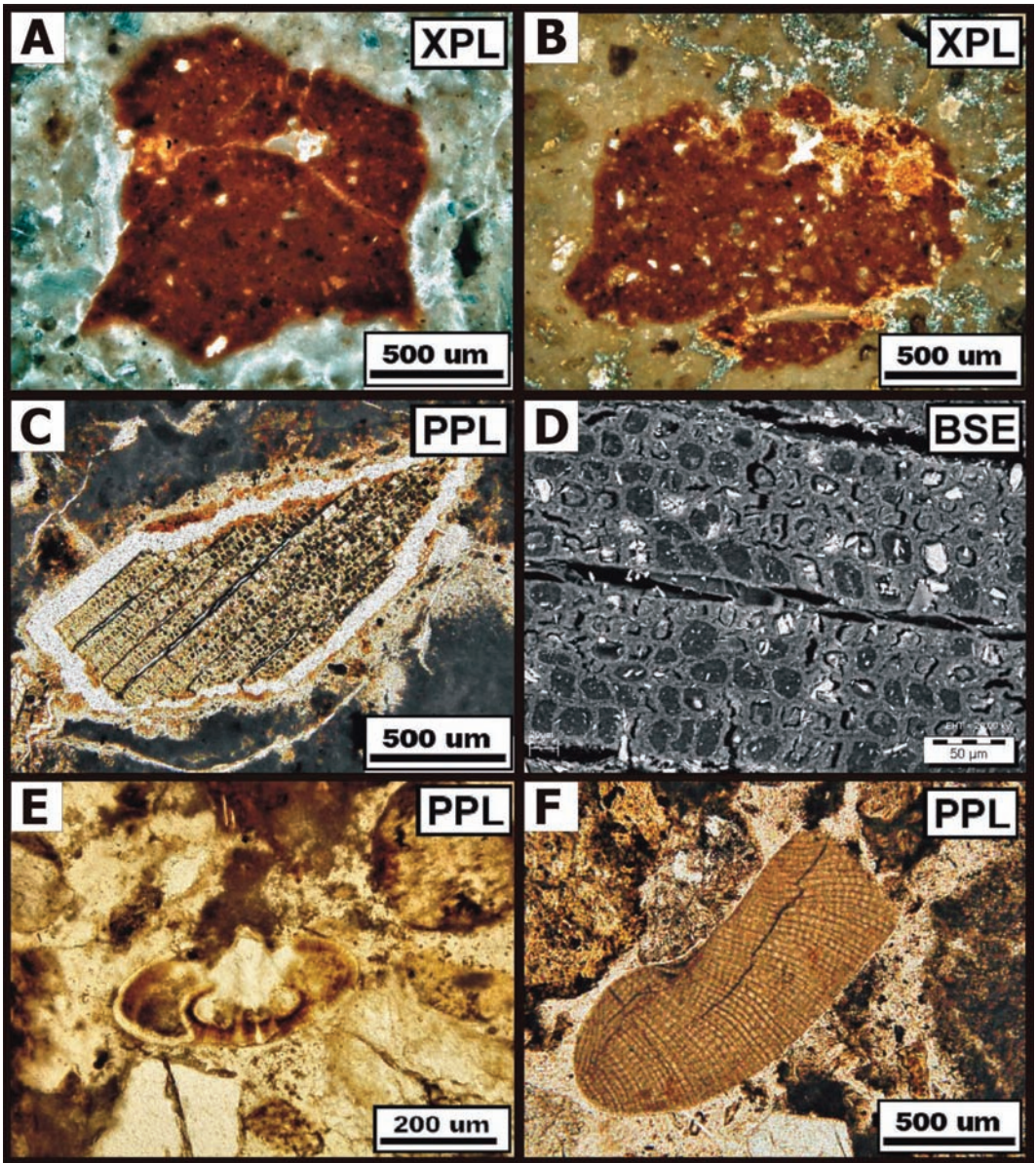
Figure 6. Characteristic diverse fine aggregate components: A-B: ceramic fragments (XPL); C-D: wood fragment probably from the original concrete framework (PPL and BSE); E: calcareous foraminifera within the mortar (PPL); F: red algae microfossil within the mortar (PPL).
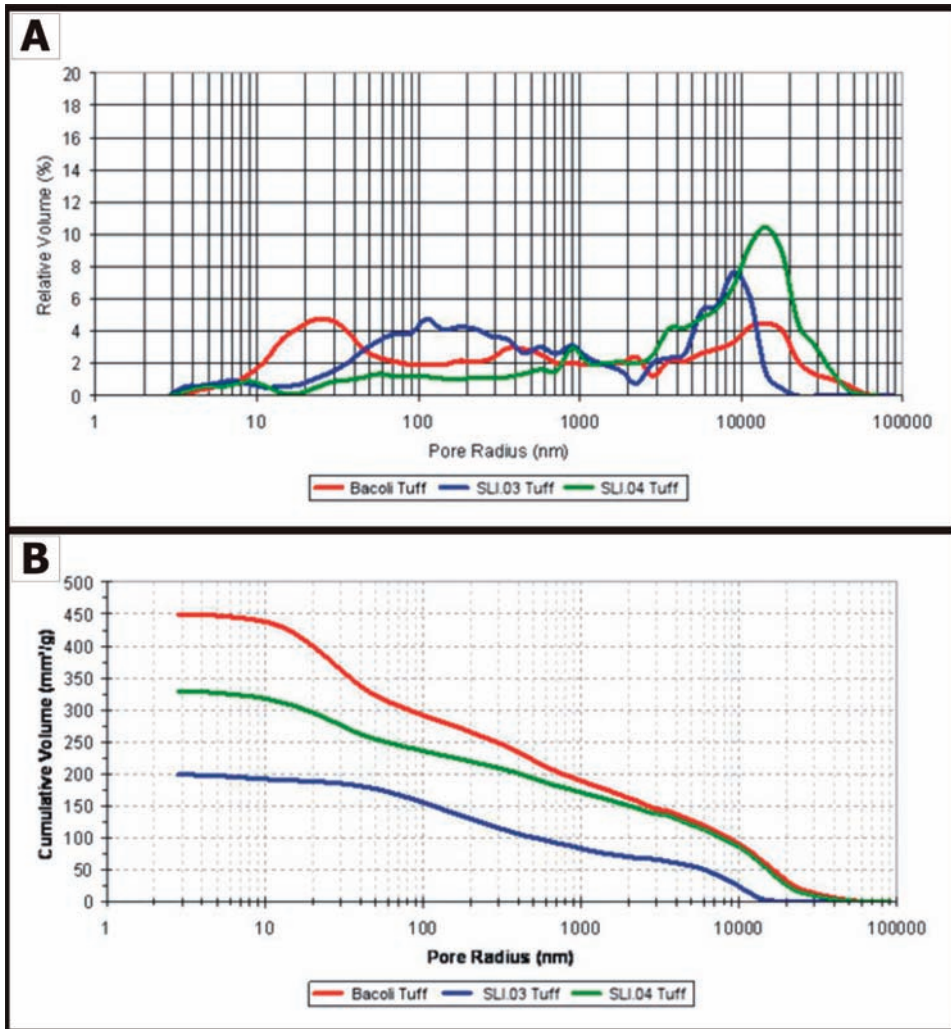
Figure 7. Mercury intrusion porosimetry of tuff-ash material from Bacoli (BAC.04) and Santa Liberata (SLI.03 and SLI.04). Plots report pore-size distributions, as relative volume (A) and cumulative volume (B).

consistent with the Neapolitan Yellow Tuff (NYT) deposit in Naples and correspond to the *pulvis Puteolanus* of Vitruvius.

Mineralogical and petrographic analysis of the cementitious binding matrix.

The cementitious binding matrix at both Santa Liberata and Caesarea is a hydraulic pozzolanic material, derived from the reaction between the lime, or maybe an hydraulic lime, and a fine-grained silicate material; taking in account that the tuff-ash aggregates at Santa Liberata and Caesarea come from the Phlegrean Fields, then it appears very probably that also the fine pozzolanic material mixed to the lime for casting both the mortars is the same material finely
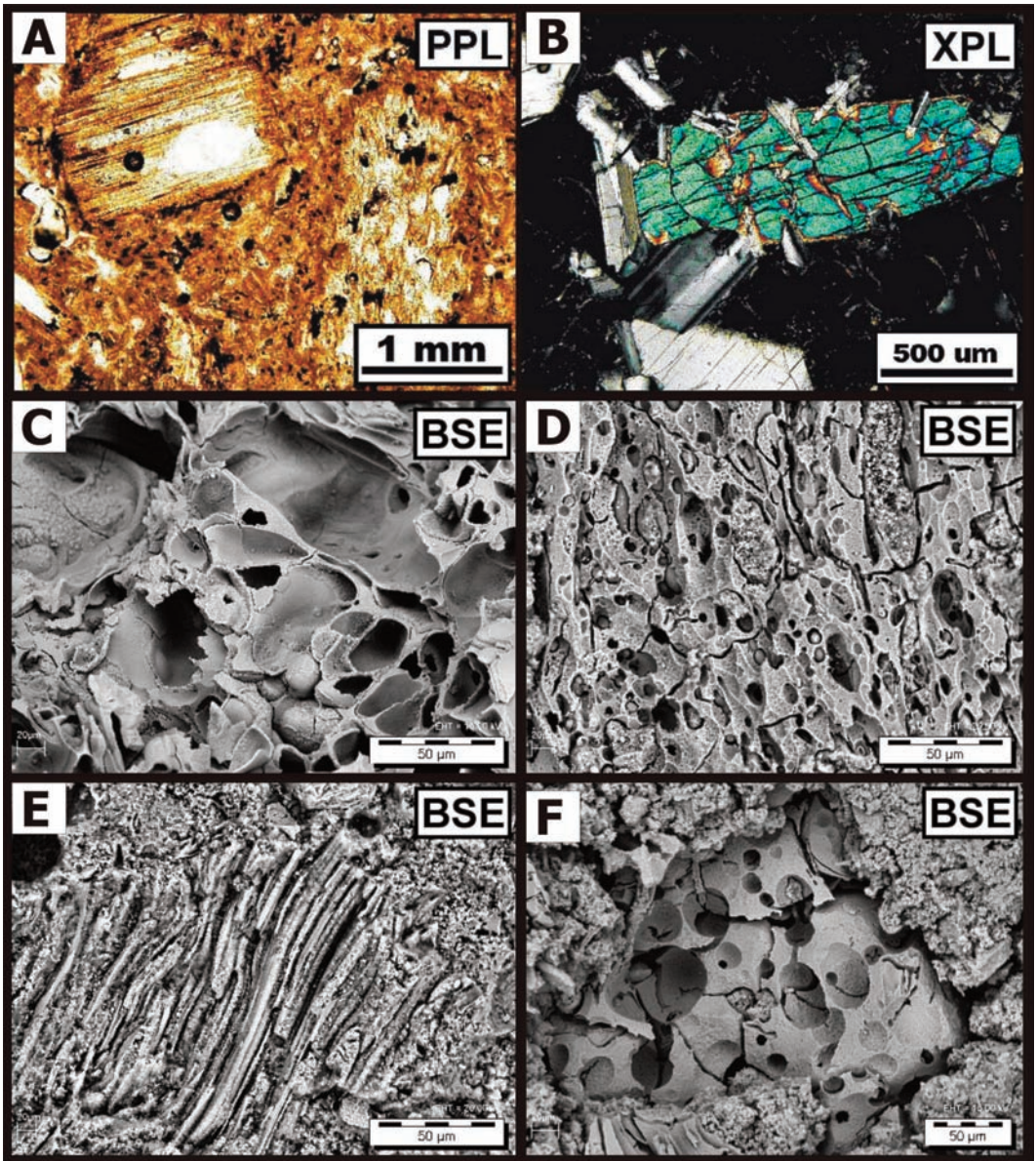
Figure 8. Characteristic components of the coarse-grained tuff-ash aggregate from quarry at Bacoli (Phlegrean Fields). A: tuff-ash texture at low magnifications shows fibrous pumice clasts cemented by a dark vitric fine ash (PPL); B: stubby clinopyroxene and K-feldspar primary phenocrysts (XPL); C-D-E-F: pumiceous vitric clasts with vesicles and fluidal texture at higher magnification (BSE images).

powdered. Hence, the cementitious binder at Santa Liberata and Caesarea with much probability was produced by the reaction of seawater with lime and the *pulvis Puteolanus* pozzolan, in variable proportions.

Petrographic examination of several thin sections, combined with SEM-EDS and XRPD analyses confirm the presence of different textures and various cements, including microcrystalline "sparry" calcite, unusual white dull clasts composed of calcite, tobermorite and ettringite, amorphous gel-like Calcium-Aluminum-Silicate-Hydrate, superficial and or interstitial crusts from salts crystallization, mostly gypsum, and finally authigenic spherical crystals with the "rosette" texture (Vola et al., 2010a). However, gel-like silica-rich C-A-S-H represents the most important hydration product, being responsible of the mechanical strength of the hydraulic binder, similar to modern cement-based materials, but richer in alumina.

Millimetric up to some centimetric-sized (4 mm-7 cm) white dull clasts of reacted lime often occur associated to microcrystalline "sparry" calcite cement (Figure 9). The composition, investigated with several XRPD analyses, consists of calcite, tobermorite $[Ca_5Si_6(O,OH)_{18} \cdot 5H_2O]$, ettringite $[Ca_6Al_2(SO_4)_3(OH)_{12} \cdot 26H_2O]$, and amorphous phase, plus metastable vaterite, brucite, and hydrocalumite, as accessories (see Table 3). Characteristic features are the fine-grained matrix at the core, and the microcrystalline reaction rim at the periphery. The former is dull, opaque, beige colored in plane polarized light (PPL), without birefringence under crossed polarizers (XPL), while the latter presents 20-40 microns sized crystals with low relief and bright first order interference colors (XPL). SEM-EDS chemical analyses attest the presence of Ca and Si (possible tobermorite) in the inner portions, whereas Ca, Al and S (possible ettringite) on the perimetral rinds (Figure 9).

White clasts from Caesarea are larger than those from Santa Liberata, and often show unusual black-and-white stripes at the mesoscopic scale (Figure 9). The preliminary hypothesis formulated by Hohlfelder et al. (2007) is that they probably formed at the initial stages of working of the mixture with the pozzolanic material and the wet lime, and consist of lumps that were chopped or mixed several time. XRPD analyses performed on a black-and-white clast, and on the white part separately, did not revel remarkable differences, because both samples were composed of calcite and a small amount of tobermorite. XRPD analyses on white clasts confirm that the main phases are calcite and/or Mg-calcite, plus subordinated tobermorite and ettringite, as well. The presence of tobermorite is considered unusual, because it generally forms during hydrothermal process as the alteration product of calcium carbonate rocks, due to contact metamorphism and metasomatism, or as an infill in vesicles and cavities in basaltic rocks, in association with zeolites, ettringite, portlandite and calcite (Anthony et al., 2003). Moreover, tobermorite can be successfully synthesized in autoclave by hydrothermal reaction at 200 °C under the pressure of 2 MPa after 3-10 hours, using an appropriated precursor (Huang et al., 2002). The presence of tobermorite within Roman pozzolanic subaerial concretes is reported in the Bridge of Augustus at Narni, close to Terni, as well (Cantisani et al., 2003). Recently, the presence of tobermorite was found in all the different ancient seawater concretes drilled by the ROMACONS team (Vola et al., 2010a; 2010b), and its formation was related to those of natural rock-forming cement systems in pyroclastic deposits immersed in the ocean and in saline lake brines (Jackson et al., 2010a). It is not clear how or if high temperatures could have been achieved, because it is well-known from the literature that the hydration heat of pozzolanic cements is lower than normal cements (Collepardi et al., 2009; Massazza, 1974; Massazza and Costa, 1979).
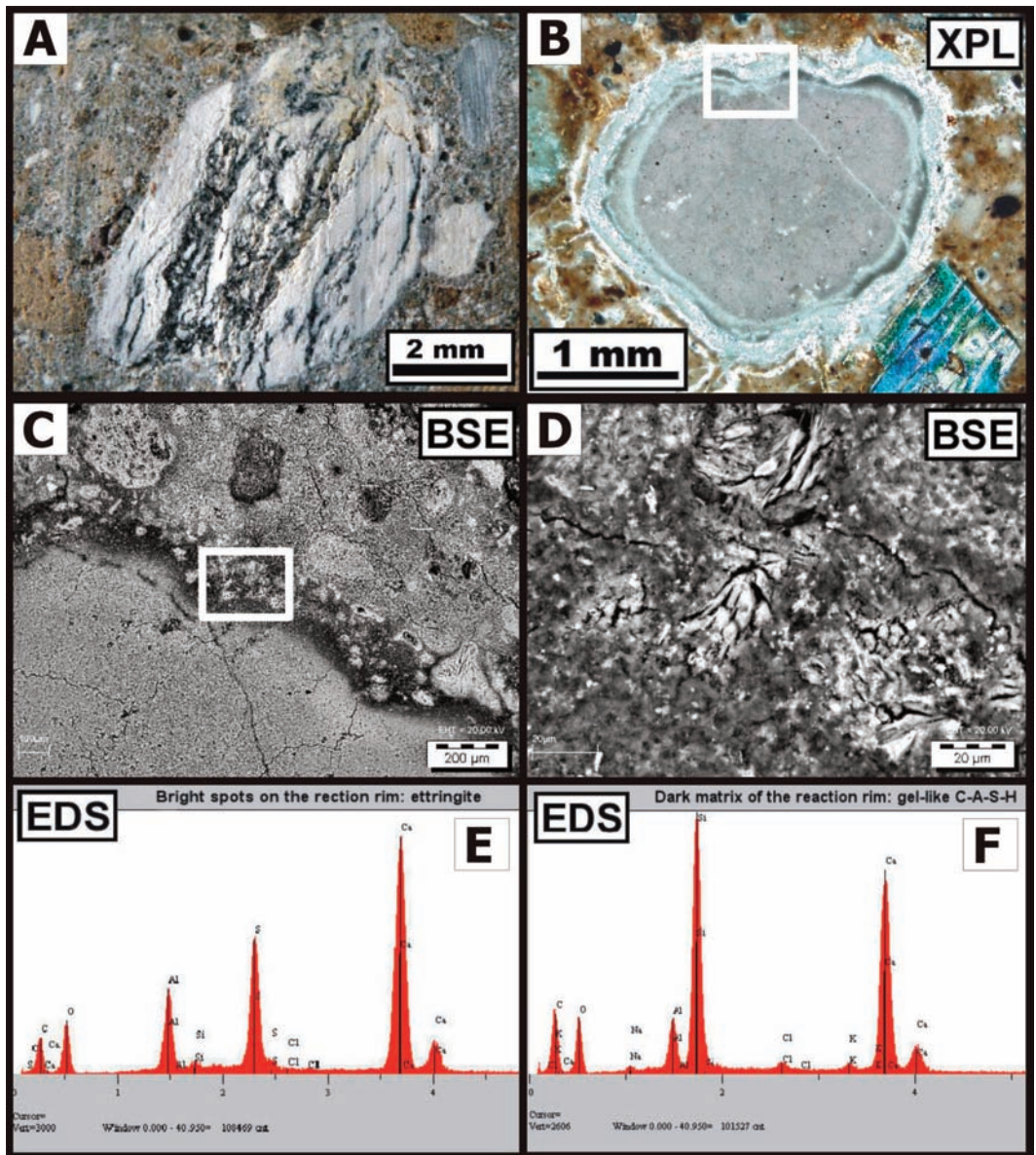
Figure 9. Distinguishing features of white clasts in SLI.04 and CAE.05. A: macrograph of "black-and-white stripes" in a white cm-sized clast in CAE.05-2; B: micrograph of a white clast in SLI.04 (XPL); C-D: reaction rim of a white clast in SLI.04 in a BSE image at low and high magnification; E: Bright dendritic spots up to 50 μm-sized, occurring within the reaction rim, are mainly composed of ettringite [$Ca_6Al_2(SO_4)_3(OH)_{12} \cdot 26H_2O$] (EDS spectra); F: dark matrix occurring around the reaction rim is mainly composed of a gel-like, silica rich, C-A-S-H (EDS spectra).

Rarely some underburned lime aggregates have been found within the Caesarea mortar. Lime is generally difficult to estimate because it reacted completely with the pozzolanic materials to form the hydraulic binder, especially the gel-like, silica-rich C-A-S-H. Underburned lime aggregates, show the original texture of a fossiliferous packstones (e.g. CAE.05-1, see Figure 10 E-F) preserved at the core, surrounded by a characteristic reaction rim. This fact may attests a provenance from a local limestone. Underburned lime aggregates were not observed in Santa Liberata.

Salts crystallization always occur within the marine concrete due to the long curing time into the seawater, which forced the penetration of sulphates and chlorides. Precipitation of dendritic gypsum, fibrous ettringite and halite crusts, within mortars extracted from broken pieces of concrete (e.g. SLI.03 medium part, and CAE.05-3), were detected by SEM-EDS chemical microanalyses (Figure 10 A-B-C-D). Moreover some accessorial cement phases, containing ions from seawater diffusion, were detected in the binding matrix using XRPD analyses. They are hydrocalumite $\{Ca_2Al(OH)_6[Cl_{1-x}(OH)_x]\cdot3H_2O\}$, hydrotalcite $\{Mg_6Al_2(CO_3)(OH)_{16}\cdot4H_2O\}$, and rarely also brucite $(Mg(OH)_2)$.

Characteristic sub-millimetric spherical crystals with the "rosette" texture, are generally widespread within the porosity of the binding matrix, as well. Distinguishing features are the radial divergent habit, low relief, and colorless in plane polarized light (PPL), low birefringence, and grey to white interference colors on crossed polarizers (XPL) (Figure 10). XRPD analyses on the mortar, combined with SEM-EDS chemical analyses on polished thin sections, identify (K, Na) phillipsite (Figure 11). "Rosette" phillipsite always shows geometrical superimposition to the other cements, attesting that it was formed in situ within the seawater concrete. From a chemical standpoint these authigenic phillipsites are consistent with those from the Neapolitan Yellow

Tuff (NYT) (de' Gennaro et al., 2000). "Rosette" phillipsite crystals may represent the last stage of crystallization within the mortar, and could be explained in terms of a metasomatic process occurring at the expense of pozzolanic glassy materials, especially tuff-ash fragments and pumiceous clasts, in an alkaline marine environment (Vola et al., 2010b).

Conclusions

Analyses performed on Roman pozzolanic concrete cores from the piers at Santa Liberata, on the Italian coast, and the breakwaters at Caesarea Palestinae in Israel, allow to identify the provenance of raw materials, the mix-design of the concrete, and products of reaction that have occurred in over two thousand years of curing in an aggressive marine environment. From a chemical standpoint, mortars from Santa Liberata and Caesarea show a similar distribution of major elements, and the soluble silica and insoluble residue ratio, coupled with the hydraulic index, widely attest that strongly pozzolanic reaction had occurred. The petrographic examination indicates that the pozzolanic tuff-ash coarse aggregate used to cast Santa Liberata concrete is the same as that at Bacoli, Naples, whereas the aggregate used in Caesarea is mainly the local *kurkar* calcareous sandstone. On the other hand, the mortars are very similar at both places, being strongly enriched with pozzolanic materials, consisting of primary tuff-ash fragments, pumiceous glassy clasts, and volcanic phenocrysts (K-feldspar and clinopyroxene) with subordinated lava fragments, black shards, and zeolites fillings (phillipsite and chabazite) as secondary alterations. This phase associations are fully consistent with those of the Neapolitan Yellow Tuff (NYT) from the Phlegrean Fields, the *pulvis Puteolanus* of Vitruvius. The cementitious binding matrix is composed of various products of reaction, including amorphous gel-like, silica-
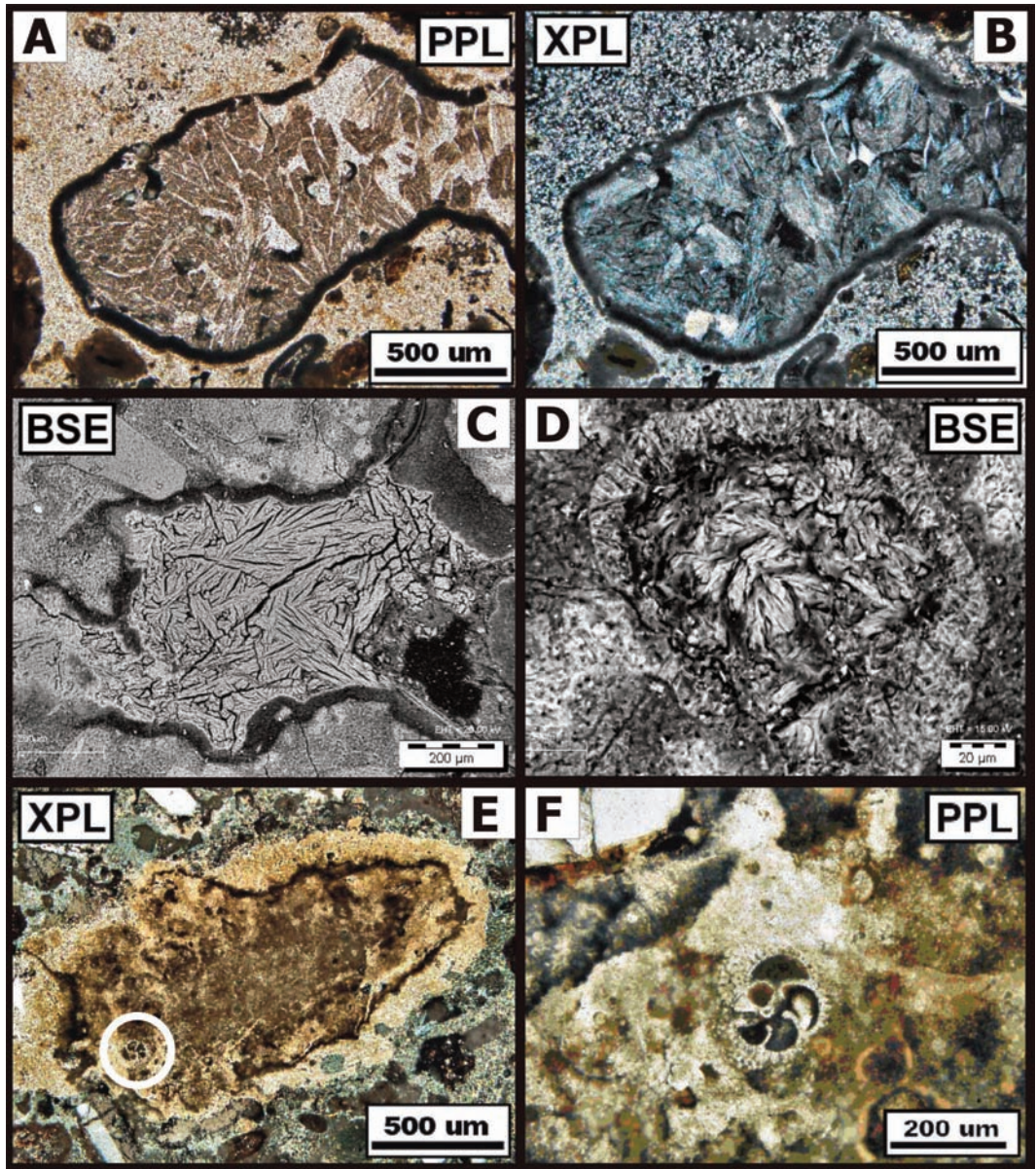
Figure 10. Characteristic typologies of cementitious binding matrix. A-B-C: dendritic sulphate encrustations, probably composed of ettringite, within the mortar's porosity in SLI.04 (PPL, XPL and BSE); D: dendritic encrustations composed of silica rich C-A-S-H gels and microcrystalline ettringite, within the mortar of CAE.05-5 (BSE); E: underburned lime aggregate from CAE.05-1 at low magnification (XPL); F: detail of a fossiliferous packstone within the previous grain at an higher magnification (PPL).
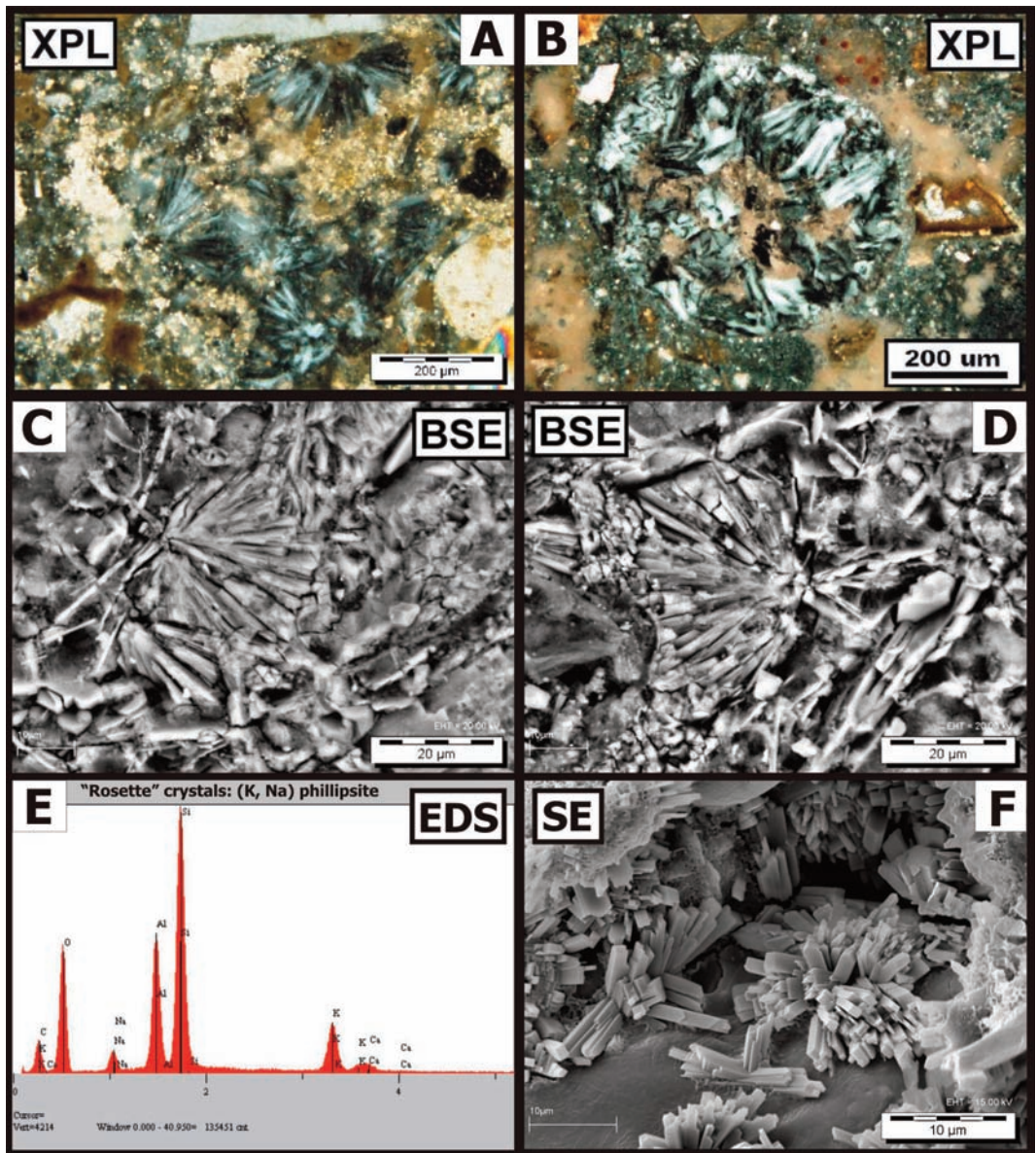
Figure 11. Distinguishing features of crystal aggregates with the "rosette" texture. A-B: authigenic spherical crystals, probably phillipsite, within the pores of the cementitious matrix of the Caesarea mortar (CAE.05) (convergent XPL); C-D-E: authigenic "rosette" crystals, composed of (K, Na) phillipsite, within the cementitous matrix of Santa Liberata mortar (SLI.04) (BSE and EDS spectra); F: phillipsite crystals on the surface of a mortar fragment in SLI.04 (SEM-SE).

rich C-A-S-H, microcrystalline "sparry" calcite, unusual white dull clasts composed of calcite, tobermorite and ettringite, encrustations derived from chloride and sulphate precipitation, and finally characteristic metasomatic spherical crystals, mainly phillipsite, with the "rosette" texture, which were probably formed in situ. Ongoing analyses, will investigate microstructural variability, related to different stages of dissolution and precipitation, and clarify their compositions, which is a key-factor in understanding the durability of ancient Roman seawater concretes.

Acknowledgements

References

Anthony J.W., Bideaux R.A., Bladh K.W. and Nichols M.C. (2003) - Handbook of Mineralogy, Volume II, Silica, Silicates. Mineral Data Publishing, 2nd Ed.

Bernardi A., De Rita D., Funiciello R. and Villa I.M. (1982) - Chronology and structural evolution of Alban hills volcanic complex, Latium, Italy, Guide-book IAVCEI, Workshop on the Explosive Volcanism, S. Martino al Cimino, Viterbo.

Bianchi E. and Meneghini R. (in press) - Nuovi dati sulle volte in calcestruzzo della Basilica Ulpia e del Foro di Traiano. *Bullettino della Commissione Archeologica Comunale di Roma*.

Bianchi E., Meneghini R., Jackson M., Brune P. and Marra F. (2011) - Archaeological, structural, and compositional observations of the concrete architecture of the Basilica Ulpia and Trajan's Forum. *Commentationes Humanarum Litterarum*, 128, 72-93.

Brandon C., Hohlfelder R.L. and Oleson J.P. (2008) - The Concrete Construction of the Roman Harbours of Baiae and Portus Iulius: The ROMACONS 2006 field season. *International Journal of Nautical Archaeology*, 37, 374-392.

Brandon C., Hohlfelder R.L., Oleson J.P. and Rauh N. (2010) - Geology, Materials, and the Design of the Roman Harbour of Soli-Pompeiopolis, Turkey: the ROMACONS field campaign of August 2009. *International Journal of Nautical Archaeology*, 39, 390-99.

Brandon C., Hohlfelder R.L., Oleson J.P. and Stern C. (2005) - The Roman Maritime Concrete Study (ROMACONS). The Roman harbour of Chersonisos in Crete and its Italian connection. *Mediterranée*, 1, 25-9.

Branton G. and Oleson J.P. (1992) - The Technology of King Herod's Harbour, in R.L. Vann (ed.): Caesarea Papers. Straton's Tower, Herod's Harbour, and Roman and Byzantine Caesarea. *Journal of Roman Archaeology*, 5, Ann Arbor MI, USA, 49-67.

Cantisani E., Cecchi A., Chiaverini I., Fratini F., Manganelli Del Fa C., Pecchioni E. and Rescic S. (2003) - Il legante del "Calcestruzzo" Romano del Ponte di Augusto a Narni, Quaderno di Leonardo 2, Leonardo Società di Ingegneria S.r.l., Basilica di Assisi, 31 Maggio 2003.

Collepardi M., Collepardi S. and Troli R. (2009) - Il nuovo calcestruzzo, Enco S.r.l., Ponzano Veneto, Grafiche Tintoretto, 5th Ed., Villorba, Treviso, 533 p.

de' Gennaro M., Cappelletti P., Langella A., Perrotta A. and Scarpati C. (2000) - Genesis of zeolites in the Neapolitan Yellow Tuff: geological, volcanological and mineralogical evidences. *Contributions to Mineralogy and Petrology*, 139, 17-35.

De Rita D., Funiciello R. and Parotto M. (1988) - Carta geologica del complesso vulcanico dei Colli Albani, Scala 1:50.000, C.N.R. P.F. Gruppo Nazionale per la Vulcanologia, Roma.

Gotti E., Oleson J.P., Bottalico L., Brandon C., Cucitore R. and Hohlfelder R.L. (2008) - A Comparison of the Chemical and Engineering Characteristics of Ancient Roman Hydraulic Concrete with a Modern Reproduction of Vitruvian Hydraulic Concrete. *Archeometry*, 50 (4), 576-590.

Hohlfelder R.L., Brandon C. and Oleson J.P. (2005) - Building a Roman Pila in the Sea. Experimental Archaeology at Brindisi, Italy, September 2004. *International Journal of Nautical Archaeology*, 34, 123-27.

Hohlfelder R.L., Brandon C. and Oleson J.P. (2007) - Constructing the Harbour of Caesarea Palestina, Israel: New Evidence From the ROMACONS Field Campaign of October 2005. *International Journal of Nautical Archaeology*, 36 (2), 409-415.

Huang X., Jiang D. and Tan S. (2002) - Novel hydrothermal synthesis method for tobermorite fibers and investigation on their thermal stability. *Materials Research Bulletin*, 37 (11), 1885-1892.

Jackson M., Deocampo D., Marra F. and Scheetz B. (2010a) - Mid-Pleistocene Pozzolanic Volcanic Ash in Ancient Roman Concretes. *Geoarchaeology*, 25, 36-74.

Jackson M. and Marra F. (2006) - Roman Stone Masonry: Volcanic Foundations of the Ancient City. *American Journal of Archaelogy*, 110, 403-36.

Jackson M., Marra F., Deocampo D., Vella A., Kosso C. and Hay R. (2007) - Geological observations of excavated sand (harena fossicia) used as fine aggregate in Roman pozzolanic mortars. *Journal of Roman Archaeology*, 20, 25-52.

Jackson M., Vola G., Oleson J.P. and Scheetz B. (2010c) - Petrographic And Chemical Maps of Pozzolanic Cement Microstructures in Ancient Roman Seawater Concretes. Geological Society of America (GSA), Denver Annual Meeting, 31 October-3 November 2010, (abs) 42, 5.

Jackson M., Vola G., Scheetz B., Oleson J.P., Brandon C. and Hohlfelder R.L. (2010b) - Chemical durability of cement systems in pozzolanic mortars of ancient Roman seawater concretes. Proc. 2nd Historic Mortars Conference (HMC2010), 22-24th September 2010, Prague, Czech Republic, RILEM, 217-225.

Jackson M., Vola G., Vsiansky D., Oleson J.P., Brandon C., Hohlfelder R.L. and Scheetz B. (in press) - Cement microstructures and durability in ancient Roman seawater concretes. In J. Valek, C. Groot and J. Hughes (Eds): Historic Mortars: Characterization, Assessment, Conservation and Repair, Springer-RILEM.

Massazza F. (1974) - Chemistry of pozzolanic additions and mixed cements. In: Proc. VI International Congress on the Chemistry of Cement (7th ICCC), September 23-27th 1974, Moscow, 1-65, esp. 4-6.

Massazza F. and Costa U. (1979) - Aspects of the pozzolanic activity and properties of pozzolanic cements. *Il Cemento*, 76, 3-18.

Oleson J.P., Bottalico L., Brandon C., Cucitore R., Gotti E. and Hohlfelder R.L. (2006) - Reproducing a Roman maritime structure with Vitruvian pozzolanic concrete. *Journal of Roman Archaeology*, 19, 29-52, esp. 47-48.

Oleson J.P. and Branton G. (1992) - The Harbour of Caesarea Palaestinae: A Case Study of Technology Transfer in the Roman Empire, Mitteilungen. Leichtweiß-Institut für Wasserbau, 117, 387-421.

Oleson J.P., Brandon C., Cramer S.M., Cucitore R., Gotti E. and Hohlfelder R.L. (2004) - The ROMACONS Project: a Contribution to the Historical and Engineering Analysis of Hydraulic Concrete in Roman Maritime Structures. *The International Journal of Nautical Archaeology*, 33 (2), 199-229.

Oleson J.P. and Jackson M. (2010) - How did expertise in maritime hydraulic concrete spread through the Roman empire? Proc. 2nd Historic Mortars Conference (HMC2010), 22-24th September 2010, Prague, Czech Republic, RILEM, 285-292.

Sneh A., Bartov Y., Weissbrod T. and Rosensaft M. (1998) - Geological Map of Israel, 1:200,000, Geological Survey of Israel (4 sheets).

UNI 6505 (1973) - Calcestruzzo indurito. Determinazione del contenuto di cemento (metodo Florentin). Norma ritirata senza sostituzione. UNI, Ente Nazionale Italiano di Unificazione.

Vola G., Jackson M., Oleson J.P., Brandon C. and Hohlfelder R.L. (2010a) - Mineralogical and Petrographic characterization of Ancient Roman Maritime Concretes from Mediterranean Harbours. Proc. 2nd Historic Mortars Conference (HMC2010), 22-24th September 2010, Prague, Czech Republic, RILEM, 381-388 (with poster).

Vola G., Stanislao C., Rispoli C., Morra V. and de' Gennaro M. (2010b) - Petrographic quantitative analysis of pozzolanic mortars from ancient Roman marine concrete cores, drilled by ROMACONS team (2006-2009). *Rendiconti Online della Società Geolologica Italiana*, 11 (2), 563-564 (with poster).